ELSEVIER

Marine and Petroleum Geology 20 (2003) 851–860

Marine and Petroleum Geology

www.elsevier.com/locate/marpetgeo

# Spatio-temporal evolution of velocity structure, concentration and grain-size stratification within experimental particulate gravity currents

W.D. McCaffrey[a,*], C.M. Choux[a], J.H. Baas[a], P.D.W. Haughton[b]

[a]*School of Earth Sciences, University of Leeds, Leeds LS2 9JT, UK*
[b]*Department of Geology, University College Dublin, Belfield, Dublin 4, Ireland*

Received 1 September 2002; accepted 28 February 2003

**Abstract**

We describe a flume study of the spatio-temporal evolution of particulate gravity currents. Time series of the vertical structure of flow in terms of the forward component of velocity, flow concentration and grain-size of suspended sediment were co-measured at a different position along the flume for each of a series of nominally identical flows. The data are combined to show the spatial evolution of a single idealised flow. Such a flow, fed into the flume from an overhead reservoir, first propagates as a quasi-steady jet. The subsequent evolution of coherent spatial and temporal trends in velocity, grain-size and concentration are developed by the internal action of the flow itself, rather than being inherited from the flow generation mechanism. Quasi-steady input currents evolved down flume into surge-type flows that wax very rapidly upon arrival then progressively wane. Thus the velocity history of currents at source may differ from that experienced downstream, indicating that flow steadiness measured (or interpreted) in downstream positions may not necessarily be indicative of the flow generation mechanism. The fore-most parts of the flow travelled more rapidly than the hind-most parts and thus gradually drew further away; as a consequence, the duration of the experimental currents systematically increased along the length of the flume (the flows 'stretched out'). Natural scale flows may therefore wane more rapidly in proximal regions than distal ones. This may impact upon sedimentation style, with higher sedimentation rates potentially more prevalent in proximal than in distal regions. Grain-size maxima are recorded in the head of the current. Convincing evidence of coarse tail lag behind the head is only patchily developed. Within the flow body a consistent pattern of upward fining then coarsening is observed. This can be related to an upward flux of coarse particles from the head, which subsequently settle downwards into the body. At the natural scale such a phenomenon may have implications for the development of coarse tail grading.


*Keywords:* Turbidity currents; Flow-structure; Flume experiments

## 1. Introduction

Experimental studies of turbidity currents commonly focus upon measurements of time series in one or more parameters (such as velocity, concentration, turbulent kinetic energy, or, more rarely, grain-size) (Best, Kirkbride, & Peakall, 2001; Garcia, 1994; Kneller, Bennett, & McCaffrey, 1997; Kneller & McCaffrey, 1999; Parker, Garcia, Fukushima, & Yu, 1987) or upon the vertical stratification in these parameters (Best et al., 2001; Garcia, 1994; Stix, 2001). A principal aim of the work detailed here is to demonstrate that although such studies may yield valuable insights into current mechanics, they do not necessarily give an accurate picture of the instantaneous longitudinal structure (i.e. the non-uniformity) of the current, nor are they directly revealing of any spatio-temporal evolution in current structure that may occur. Uniformity is a measure of spatial variation in flow structure: uniform flows do not vary spatially, whereas non-uniform flows do. This can be contrasted with steadiness, which is a measure of the variations in flow structure, in which steady flows do not vary temporally, unlike unsteady flows. Allen (1985) provides definitions of uniformity and non-uniformity, steadiness and unsteadiness; Kneller and Branney (1995) adopt and expand these definitions, particularly with respect to velocity non-uniformity.

At present, time series measured within gravity currents are commonly interpreted in terms of the longitudinal

* Corresponding author. Tel.: +44-223-233-6625; fax: +44-233-5259.
*E-mail address:* mccaffrey@earth.leeds.ac.uk (W.D. McCaffrey).

0264-8172/$ - see front matter © 2003 Elsevier Ltd. All rights reserved.
doi:10.1016/j.marpetgeo.2003.02.002

current structure (e.g. Best et al., 2001; Kneller et al., 1997; Kneller & McCaffrey, 1999). For example, Kneller et al. (1997) and Kneller, Bennett, and McCaffrey (1999) conducted time series analysis of lock-exchange-generated, solute-driven gravity currents by taking measurements within the head during the phase in which its propagation velocity was quasi-steady (e.g. Simpson, 1997 and references therein). Although different components of turbidity current can be studied in this way, if the current is non-uniform, its overall longitudinal structure cannot be analysed using data collected at a single position. This is because the structure of any particular region (such as the head) measured at one time cannot be compared directly with the structure of another region (such as the body) measured at a different time unless the spatial rate of change of the current is small, or zero, such that the structure of any particular region is essentially the same irrespective of the measurement position. This condition is unlikely to be achieved in practice because most turbidity currents are non-uniform along their length (even in the absence of bathymetric effects) because of deposition and/or entrainment of sediment and/or fluid. An exception might be steady, river-derived hypopyncal flows (e.g. Mulder & Syvitski, 1995; Mulder, Syvitski, Migeon, Faugeres, & Savoye, 2003), where the rates of entrainment and detrainment of water and/or sediment are negligible.

In this paper, a comprehensive experimental study of the spatio-temporal evolution of particulate gravity current structure is described. The resultant data are thought to be unique in that:

1. Time series showing the vertical stratification in horizontal velocity, flow concentration and grain-size distribution are co-measured for the first time, enabling the links between these parameters to be evaluated.
2. The methodology allows both the spatial and temporal evolution in these parameters to be evaluated: the data from nominally identical flows measured at separate locations being combined to give the spatio-temporal evolution of a single idealised flow. Various sedimentological implications of this flow evolution are investigated.

## 2. Experimental set-up

### 2.1. Flow generation, flume geometry and instrumentation

A series of eight nominally identical experimental flows were run. They comprised silica flour suspensions of initial concentration 5% by volume and mean grain-size ~8 μm (Fig. 1). In each run, 30 l of suspension were prepared in an overhead reservoir (method after Best et al., 2001) and continuously stirred to ensure uniformity. A sealing stopper was released to allow the suspension to drain (in about 25 s) via a 63 mm diameter connecting pipe into a flume 10 m long and 0.3 m wide, water-filled to a depth of 0.3 m (Fig. 2). The tank was instrumented with siphons, which sampled the flows continuously, and with 4-MHz ultrasonic Doppler velocity profiling (UDVP) probes, oriented to record the downstream component of horizontal flow velocity (technique after Best et al., 2001 and references therein). Individual UVDP probe sampling rates are a function of the number of probes multiplexed together; they were around 26 Hz for the six-probe arrays described below. Siphon samples were collected at a frequency of 0.25 Hz for all but Flow 8, which was sampled at 0.8 Hz. The siphon samples were processed using a Malvern Mastersizer Plus laser diffraction grain-sizer (measurement range 0.05–550 μm) to yield both concentration and grain-size data. Because the sampling process is intrusive, each flow could be sampled at one location only. The inbound flows were eventually reflected from an overflow weir (Fig. 2), travelling upstream as trains of solitary waves (e.g. Edwards, 1993; Pantin & Leeder, 1987). Data collected after the arrival of these waves were not analysed. Because the suspension entered the flume from an overhead reservoir, the counterflow across the upper surface of the flows common to shallow lock-exchange configurations was minimised (see Peakall, Felix, McCaffrey, & Kneller, 2001 for a discussion of this approach).

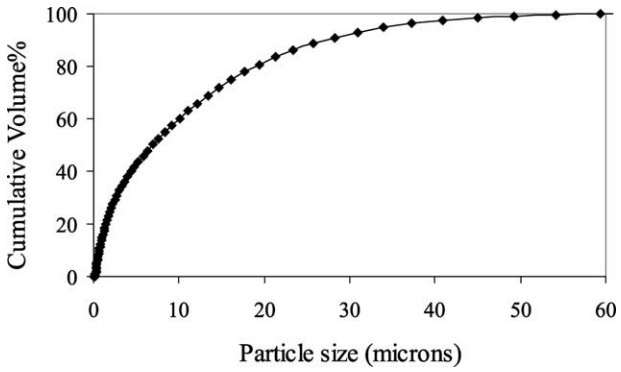


Fig. 1. Silica flour grain-size distribution.

### 2.2. Experimental programme

Flows 1 and 2 were measured at the reservoir outlet in order to establish accurately the duration of the inbound flow and its steadiness in terms of velocity, grain-size and concentration. A single siphon/UDVP pair was centred on the outlet tube, some 0.04 m downstream of its termination. Flows 3–8 were designed to measure spatio-temporal flow evolution. Each of these flows was siphoned continuously at heights 0.6, 1.6, 2.6, 3.6, and 4.6 cm above the flume floor. Simultaneously, six 4-MHz UDVP probes recorded the downstream component of horizontal flow velocity. All but the highest probe (height 7.6 cm) were positioned at the same height as the siphons. The measurement rake of co-mounted UDVP probes and siphons remained fixed,

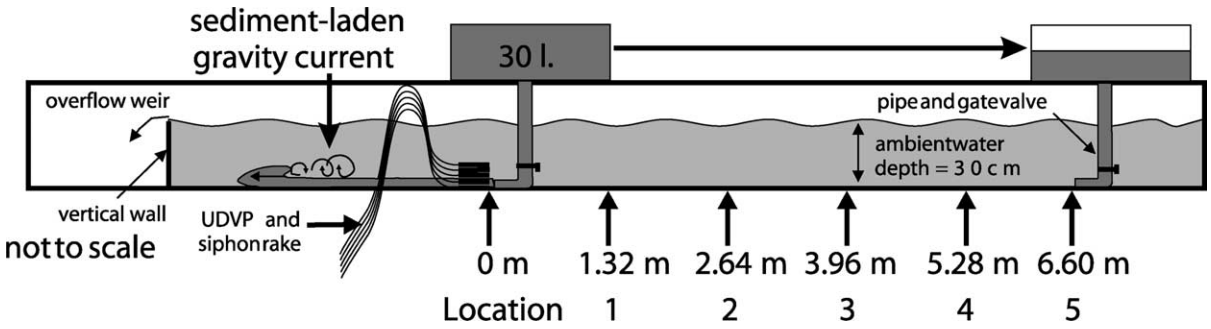


Fig. 2. Experimental set up.

whilst between each run the reservoir was moved upstream in 1.32 m increments in order to vary the distance between the sampling location and the inlet (Fig. 2). Flows 3–7 were sampled at positions located 1.32, 2.64, 3.96, 5.28 and 6.60 m from the inlet, hereafter called Locations 1–5, respectively. Flow 8 was measured at Location 3, as above, but with the siphon sampling rate increased from 0.25 to 0.8 Hz in order to optimise data collection from the front of the current. An image of the head of Flow 8 at Location 3, 3.96 m downstream from the inlet, is shown in Fig. 3.

## 3. Experimental data: description

The experimental data were processed to show time series in the vertical structure of the flow in terms of horizontal velocity, median grain-size and concentration (Figs. 4–6). The data were also processed to show the spatial evolution of a single idealised flow (Fig. 7). Fig. 5 shows grain-size and concentration data from a repeat flow (Flow 8) taken at Location 3.

### 3.1. Input condition

Flows 1 and 2 were designed to assess the steadiness of the input condition. The input was quasi-steady in terms of velocity, concentration and mean grain-size for some 22 s after flow initiation before the flow rapidly waned as the reservoir emptied (Fig. 4). Slight differences in mean grain-size between the two runs were observed. The average concentration at this location (0.04 m downstream of the inlet) was 2.5 vol%. Measurement of the reservoir concentration preceding release of Flows 1 and 2 confirmed that the initial suspension was 5% by volume. At the inlet, Reynolds and Froude numbers are calculated to be $8 \times 10^4$ and 0.6, respectively, indicating that the flow was both fully turbulent (by the criteria of Massey, 1989) and sub-critical.

### 3.2. Velocity data

The evolution of the spatial pattern of horizontal velocity is shown in Fig. 5A. In all but Location 1, the velocity maximum is located approximately one-third of the way up from the base of the flow for both the head and body of the current. The height of the velocity maximum (2–3 cm) does not appear to vary with time within the resolution of the measured heights, apart from at Location 1, where it appears to rise from 2 to 3 cm over approximately the first 10 s after the arrival of the current. Insufficient data were collected from below the velocity maximum to allow calculation of shear velocities.

At every sampling location, the currents exhibit a straightforward history of a rapid increase in velocity associated with the arrival of the current, followed by

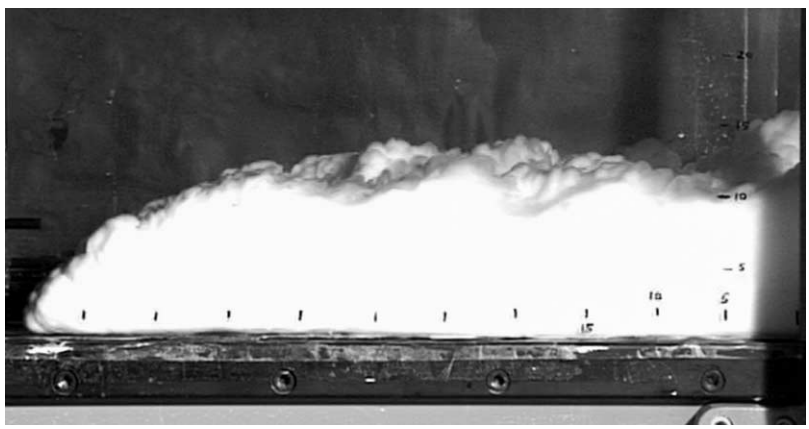

Fig. 3. Frame grab from digital video of the head of Flow 8, measured at Location 3, 3.96 m downstream from the inlet. Field of view is approximately 55 cm wide.

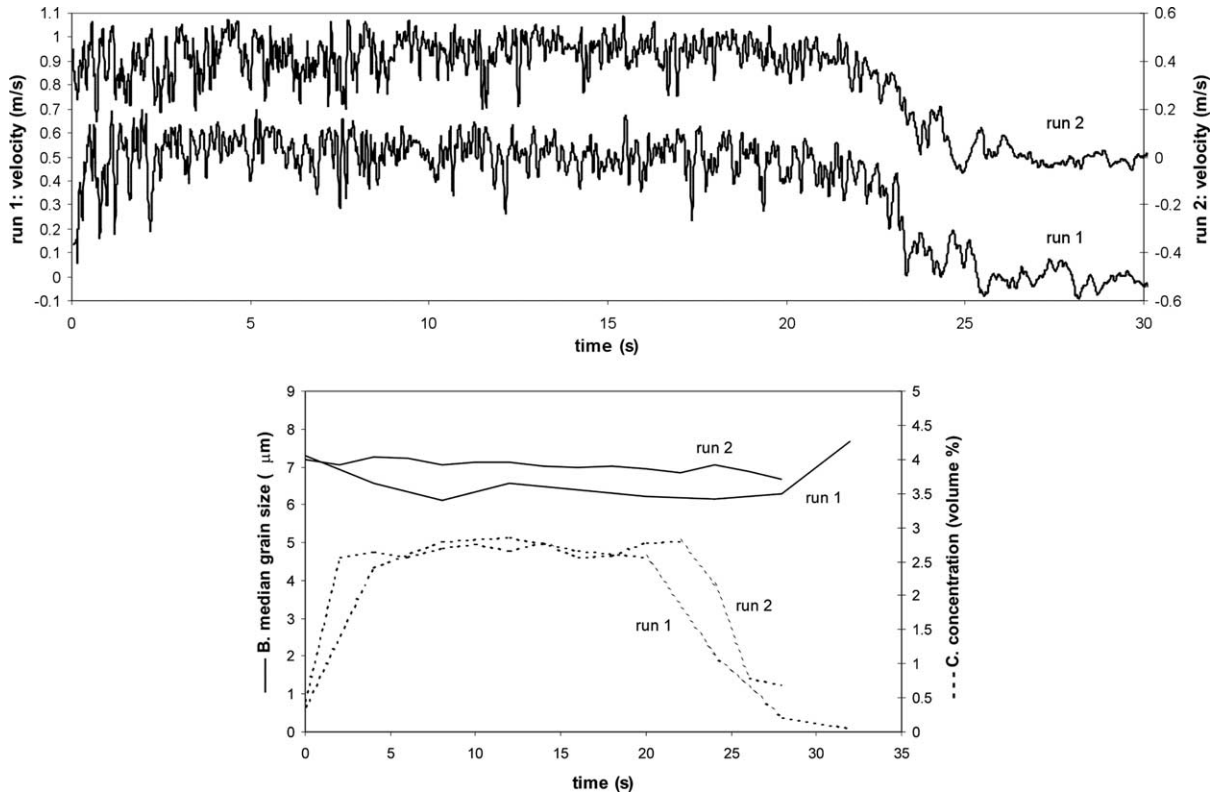


Fig. 4. Time series of Flow 1 measured at the inlet. (A) Horizontal velocity (mm $s^{-1}$). (B) Median grain-size (μm). (C) Concentration of suspended particles (vol%). Note: the horizontal velocity was measured within the inlet tube, some 30 mm from its end. Median grain-size and flow concentration are based on measurements taken from a siphon positioned some 0.04 m downstream of the end of the inlet tube.

a gradual reduction in velocity (i.e. a waning flow velocity signature). It should be noted that small upstream velocities were measured at the highest probe just before arrival of the current, although their magnitudes were too small to be represented in Fig. 5A. Peak horizontal velocities exceed 175 mm $s^{-1}$ at Locations 1 and 2, but decrease to between 150 and 175 mm $s^{-1}$ at more distal locations. It should be noted that the currents were reflected from the overflow wier, the reflected flow passing over the measurement site before the obverse current had completely come to rest. For this reason, the time taken for the horizontal flow velocity to fall below a nominated value was used as an indication of current duration. By this measure, flow duration progressively increased downstream. For example at Location 1, the lag time for the horizontal velocity to return to 50 mm $s^{-1}$ after the arrival of the head was 30 s; this increases to 34, 41, 42.5 and 48 s at Locations 2–5, respectively.

### 3.3. Grain-size data

Figs. 5B and 6A show that an apparently coherent structure developed in terms of the grain-size distribution of the suspended material. At all sampling locations, the coarsest grain sizes were recorded immediately after the arrival of the current. Within this region, which corresponds approximately to the first 4 s of the current, mean grain-size coarsens then fines upwards, with the maximum mean grain-size recorded at approximately the same height as the velocity maximum. Maximum mean grain sizes within this region of the current progressively decrease from 8 μm at Location 1 to 7.6, 7.6, 7.3 and 6.8 μm at Locations 2–5, respectively. Some 4 s after the current arrival, a rapid decrease in mean grain-size of the order of 1 μm is observed. At the most proximal location, Location 1, the subsequent flow apparently weakly coarsens upwards. In the other, more distal positions, the lower parts of the subsequent flow fine upwards, then coarsen upwards. Thus a grain-size minimum is developed within the flow, the height of which becomes progressively lower with time at each of Locations 2–5.

### 3.4. Concentration data

The temporal evolution of concentration at each of the sampling locations is shown in Fig. 5C (see also Fig. 6B). At all locations and times, concentration progressively diminishes upwards. The maximum concentration is, however, recorded some 20–25 s after the arrival of the flow. The absolute values of concentration diminish markedly between the most proximal Location 1 and Location 2, with a drop in the maximum recorded concentration from 4 to 2.25 vol%. Thereafter, the rates of decrease of concentration are much lower. In addition, the heights of individual concentration contours are

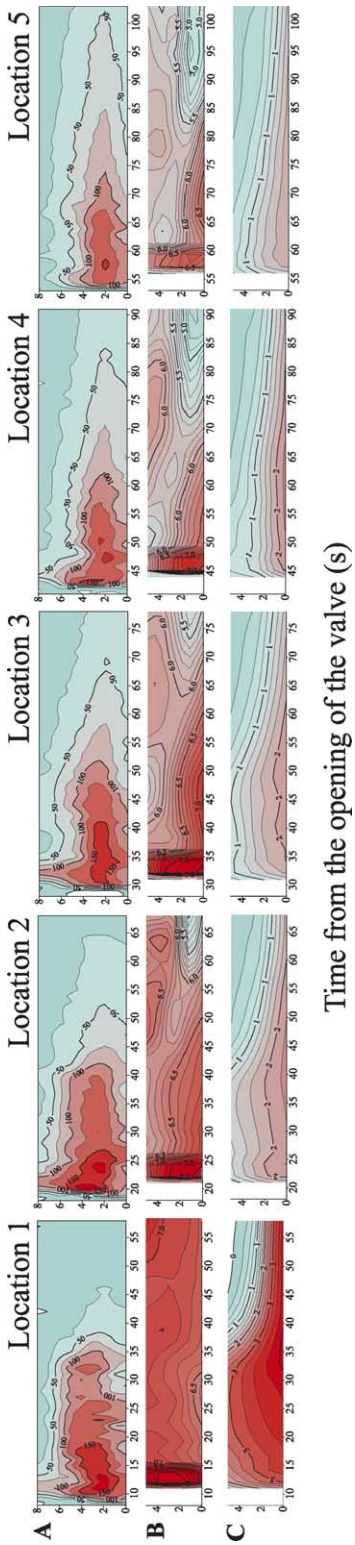


Fig. 5. Flows 3–7: time series at heights 0.6, 1.6, 2.6, 3.6, 4.6 and 7.6 cm within the flow measured at Locations 1–6 (i.e. 1.32, 2.64, 3.96, 5.28 and 6.60 m, respectively, from the inlet point). (A) Horizontal velocity (mm $s^{-1}$). (B) Median grain-size (μm). (C) Concentration of suspended particles (vol%). Note: the raw velocity data were averaged to yield sample rates equivalent to the 0.25 Hz rates obtained for the grain-size and concentration data.

generally observed to be lower at successive sampling positions. The 2.25 vol% contour is present at the base of the flow at Location 2, is absent at Location 3, re-appears at Location 4 and is absent, once again, at Location 5.

## 4. Experimental data: interpretation

### 4.1. Input condition

The relative steadiness of the input illustrates that the subsequent evolution of temporal trends in velocity, grain-size and concentration as described above are inherent to these experimental flows, being developed by the internal action of the flows themselves, rather than inherited from the flow generation mechanism. It should be noted that slight differences in mean grain-size between Flows 1 and 2 were observed, indicating that Flows 3–8 also may not have been entirely identical at initiation. However, the coherency of the patterns of grain-size distribution developed and the progressive nature of proximal to distal changes observed suggest that these differences do not strongly influence the spatial variations in flow evolution at this scale of observation. The similarity between Flow 5 and Flow 8 data measured at Location 3 (Figs. 5 and 6) also suggests that flow reproducibility is reasonable. The 50% reduction in suspension concentration from 5% by volume in the reservoir to 2.5% by volume as measured in the flume within Flows 1 and 2 (i.e. 0.04 m from the inlet) is interpreted to be a flow dilution effect, relating to ambient water entrainment.

### 4.2. Velocity data

The arrival of the head can be recognised by the rapid increase in horizontal velocities seen at all but the highest sampling height and at every sampling location. The small upstream velocities recorded at the uppermost UDVP probes (not represented on the velocity plots) are interpreted to represent movement of ambient fluid over and behind the head. The transition from head to body is less straightforward to identify at or below the velocity maximum, but can be recognised above this level by the relatively rapid decrease in velocities observed. This means of identifying the head corresponds quite closely with methods based on grain-size or concentration data (see below).

Flow duration progressively increases downstream. This is interpreted to be caused by the front-most parts of the flow travelling more rapidly that the hind-most parts and thus gradually drawing further away (i.e. the current becomes ‘stretched’). This behaviour is observed in the output both of simple box models and more complex numerical models of turbidity currents (e.g. Dade & Huppert, 1995; Felix, 2001). Consequently the current wanes more rapidly in proximal positions then in distal ones (see also Kneller & McCaffrey, 2003).

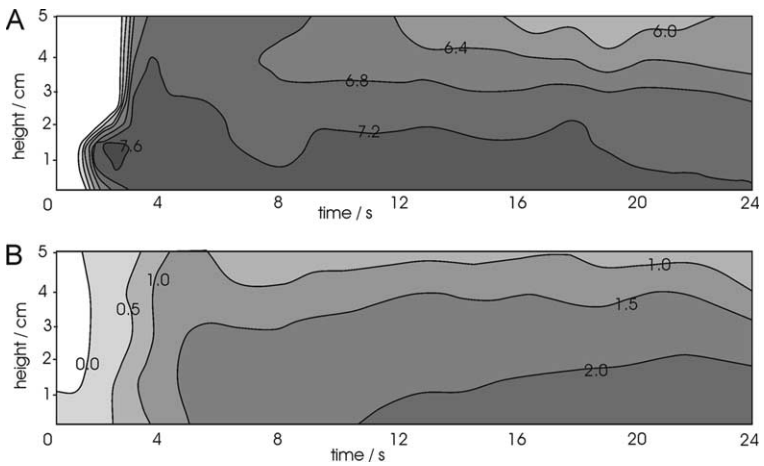


Fig. 6. Flow 8: time series at height 0.6, 1.6, 2.6, 3.6, 4.6 and 7.6 cm within the flow measured at Locations 3 (i.e. 3.96 m from the inlet point). (A) Median grain-size (μm). (B) Concentration of suspended particles (vol%). Note: (1) The siphon sample collection rate was 1.2 Hz for this flow.

### 4.3. Grain-size data

Figs. 5B and 6A show that a distinct and coherent structure is developed in terms of the grain-size distribution of the suspended material. Although the measured size range of suspended material is small (some 2 μm), the coherency of the observed patterns (and the apparent reproducibility of the grain-size trends as measured at Location 3) suggests that the measured variations are real, and do reflect the evolving flow structure.

The grain-size data permit the passage of the head of the current to be recognised as the ~4 s interval after the arrival of the current, and before the rapid 1 μm decrease in mean grain-size. It is interesting to note that the measurement of

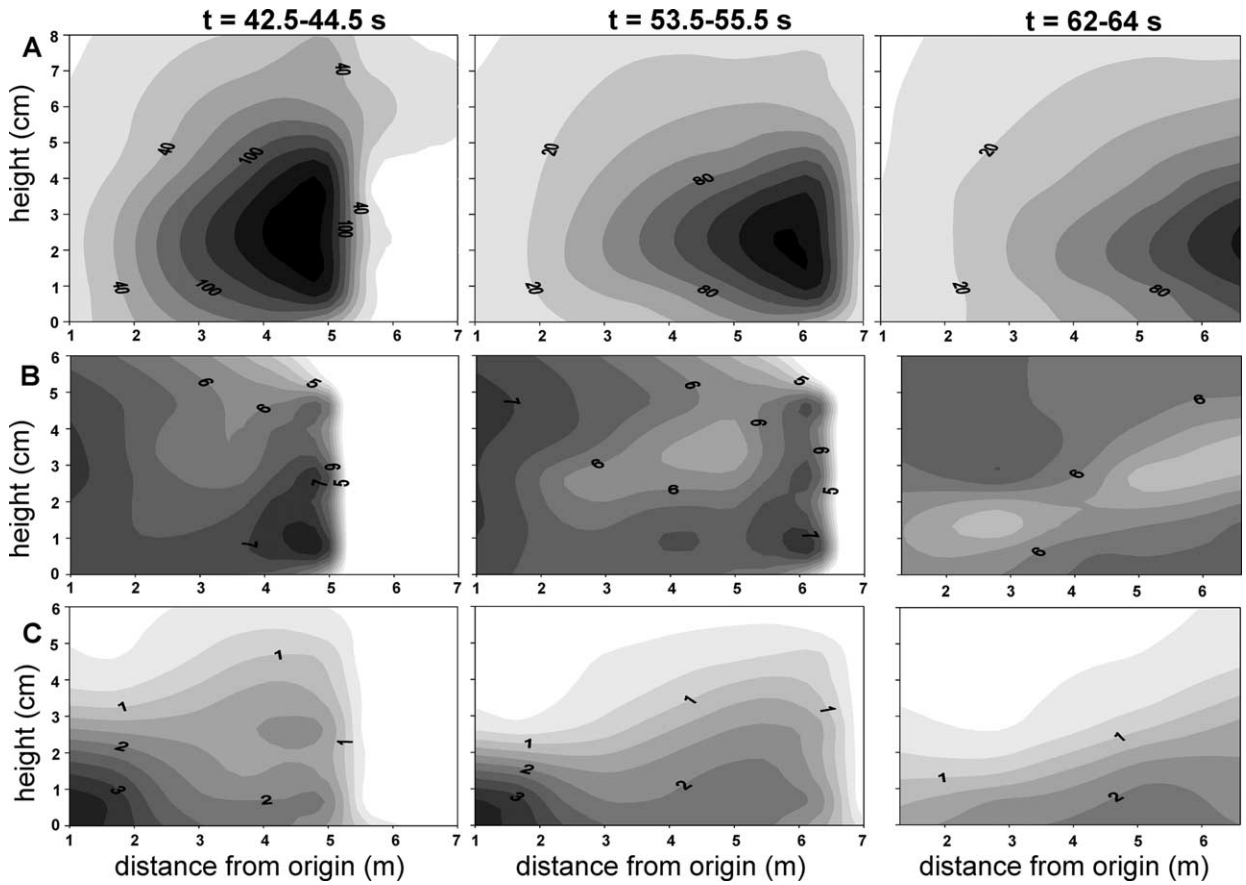


Fig. 7. Spatio-temporal evolution of a single idealised flow in terms of (A) horizontal velocity (mm $s^{-1}$), (B) median grain-size (μm) and (C) concentration (vol%), shown at intervals 42.5–44.5, 53.5–55.5 and 62–64 s after initiation, and produced by combining data from Flows 3–7.

grain-size maxima within the head is contrary to patterns of longitudinal grain-size distribution that might be anticipated through the application of simple Rouse-type sediment suspension models (e.g. Hand, 1997; Middleton & Southard, 1984). In these models, the suspended grain populations of turbidity currents bearing mixed sediment types are thought to be vertically differentiated, with faster-settling grains preferentially concentrated relatively lower in the flow, and slower settling grains relatively more evenly vertically distributed. Hand (1997) concluded that because the coarsest tail of the suspension was preferentially carried at a height below the velocity maximum, it would lag behind the head during transport. There is no evidence of coarse tail lag in these experiments, except between 37 and 46 s in the two time series of grain-size measured at Location 3 (Flows 5 and 8, Figs. 5B and 6A, respectively), and between 61 and 68 s in that measured at Location 5 (Flow 7, Fig. 5B). However, the basal siphon probe was centred some 0.6 cm above the flume floor, and it is possible that lag of coarser material may have occurred beneath this level, conceivably as bed load.

The inverse grading seen within the body may be linked to coarse particles in the head being swept upwards and backwards, then falling back into the tail of the current. In the absence of vertical velocity data, this interpretation cannot be directly verified using this data set. However, if the upward transition to coarser grain sizes represents a transition into a zone populated by coarser grains falling from suspension, this could account for the minimum grain-size zone becoming progressively lower with time. An alternative is that body turbulence in the upper part of the flow may have inhibited the settling of coarse particles. This interpretation is not preferred, as the coarsening-upward pattern is not seen in the highest velocity parts of the time series.

### 4.4. Concentration data

Although differentiation of the head and body of the flows is best achieved using the velocity and grain-size data (see above), the concentration data allow the body–tail transition to be identified—it can be recognised as a variably well-developed concave-up kink on the concentration contours on the height–concentration plots (Fig. 5C).

The increase in concentration from a mean of 2.5 vol% at the inlet to a maximum recorded value at Location 1 of 4% (recorded at the base of the flow) is interpreted to result from deposition from the current. The abrupt change in concentration observed between Locations 1 and 2 suggests that the flow was essentially continuing to collapse between these points, and was thus probably characterised by relatively high rates of ongoing sedimentation. This process may account for the development of concentration maxima some 20–25 s after the arrival of the head at Locations 1 and 2, the delay corresponding to the mean time taken for particles to fall from suspension into the lowermost regions of the flow before being deposited. Beyond Locations 1 and 2 the current generally becomes progressively more dilute downstream, presumably due to ongoing sedimentation and water entrainment. The re-appearance of the 2.25 vol% contour in the time series measured at Location 4, noted above, may possibly relate to variation in the starting condition. A slightly finer grained suspension would have produced a flow subject to lower rates of sedimentation (e.g. Bonnecaze, Huppert, & Lister, 1993; Gladstone, Phillips, & Sparks, 1998; Imran & Parker, 1999).

### 4.5. Spatial flow evolution

The data from the five nominally identical flows as measured at Locations 1–5 can be combined to illustrate both the temporal and spatial evolution of a single idealised flow in terms of horizontal velocity, grain-size and concentration (Fig. 7). It should be noted that the data collected after the passage of flow reflected from the tank end-wall are not represented. It is clear that these experimental flows are highly spatially non-uniform (i.e. they are highly depositional, despite the use of a relatively fine grained and non-cohesive material—8 μm silica flour—as a sediment analogue). Analysis of the grain-size and concentration plots highlights the potential hazards of interpreting the time series in terms of longitudinal flow structure. For example, time series of grain-size at Location 3 (Figs. 5B and 6A) indicate coarse tail lag behind the head, whereas no such trends are seen in Fig. 7. However, the occurrence of a grain-size minimum zone whose height progressively decreases along the length of the current can be recognised.

## 5. Scaling

In these experiments, a Froude scaling approach was adopted (e.g. Peakall, Ashworth, & Best, 1996). Thus the criticality state of the experimental and natural scale analogue flows must be the same (subcritical in this case). Flow Reynolds numbers in both the experimental and natural scale analogue flows must remain within the turbulent regime. Reynolds numbers of the experimental flows were calculated to be of the order $8 \times 10^4$ at the inlet. Flow is generally considered fully turbulent at flow Reynolds numbers of 2000 or above (e.g. Massey, 1989). However, Parsons and Garcia (1998) concluded that Reynolds numbers should exceed $Re \approx 2 \times 10^5$ if the energy cascade is to be preserved across all scales of turbulence, implying that these experiments most accurately model the depositional regimes of natural scale currents. Grain-size scaling was achieved by scaling grain terminal settling velocity with the body velocity of the flow. On this basis, the experimental flows might equate to natural scale flows with body velocities of the order of $5\ m\ s^{-1}$, depositing very fine sand.

## 6. Implications for the rock record

It is interesting to note that experimental currents that initiated as quasi-steady input (albeit limited duration) flows developed a simple surge structure. Thus the steadiness histories of these flows do not reveal the initial state of the currents, and hence the flow generation mechanism. At the natural scale, therefore, the history of turbidity current steadiness as evidenced, for example, in the vertical grading structure of a deposit, may not necessarily be indicative of the mechanism that generated the flow, at least for short duration events (see also Kneller & McCaffrey, 2003).

The length (and hence duration) of the experimental currents systematically increases along the length of the flume. In natural turbidity currents, this indicates that the steadiness history of a flow may vary along the length of its distribution pathway, with, for example, a more rapid decline in velocity being experienced in proximal areas compared to relatively more distal areas (Fig. 8). In natural flows, this implies that the overall duration of sedimentation may be relatively short in proximal regions compared to distal regions. In turn this may influence the style of sedimentation, with capacity-driven deposition (sensu Hiscott, 1994) relatively more prevalent proximally, and competence-driven deposition relatively more likely distally. One consequence would be that massive beds might be more likely to be developed proximally, with beds exhibiting traction structures more likely to be deposited distally (e.g. Kneller & McCaffrey, 1999; Lowe, 1982).

In these experiments grain-size maxima were recorded in the head. There is no evidence of coarse tail lag, except between 37 and 46 s in the two time series of grain-size measured at Location 3 (Flows 5 and 8, Figs. 5B and 6A, respectively) and between 61 and 68 s in that measured at Location 5 (Flow 7, Fig. 5B). On the assumption that turbidite beds build via progressive aggradation, Hand (1997) concluded that coarse tail lag behind the head during transport potentially results in the deposition of a thin inverse-graded interval at the base of otherwise normally graded deposits. Although the experimental deposits were not examined, we argue that they should show a vertical structure that principally relates to the time series in grain-size at the base of the flow. On this basis, inverse grading might be anticipated in sediments deposited around Locations 3 and 5, but not necessarily at the base of the deposit. The head would have to be entirely non-depositional in order to produce inverse grading from the base upwards. It follows that the passage of similarly structured currents at the natural scale might potentially result in complex vertical grading patterns in any resultant deposits.

The coarsening-upwards seen within the upper parts of the bodies of the flows is interpreted to relate to coarse particles in the head being swept upwards and backwards, then falling back into the body and tail of the current. In depositional currents, these grains are likely to fall through the current to the bed more rapidly than the relatively finer material in the body. In these experiments, however, the time series indicate that this wave of coarser grains would not have reached the bed until late in the history of the flows' passage. It can be inferred that a coarsening-upwards interval is likely be developed towards the top of the deposit in these cases; this is the subject of ongoing investigation. At the natural scale, however, the coarser grains could be deposited at the same time as finer material coming straight out of suspension from the body of the flow, to produce coarse tail grading patterns superimposed on more subtle (distribution) grading patterns of a relatively finer grained matrix. The grading of the coarse tail would arise because the coarsest grains would reach the bed first. Timing differences in the onset of deposition of these separate components of the suspension would lead to differences in the vertical structure of the deposit. Where sedimentation of both head- and body-derived components begins synchronously, classic coarse tail grading might be developed (Fig. 9A). If there were a lag time between deposition directly from the body and the first arrival at the bed of coarser, head-derived material, it is

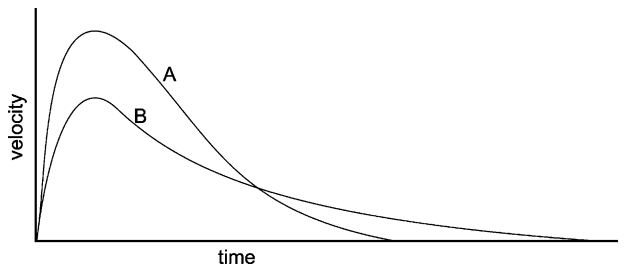


Fig. 8. Hypothetical depth-averaged time series in mean horizontal velocity for the same flows at relatively proximal and relatively distal positions. The effective rate of decline of velocity is greatest at the more proximal location.

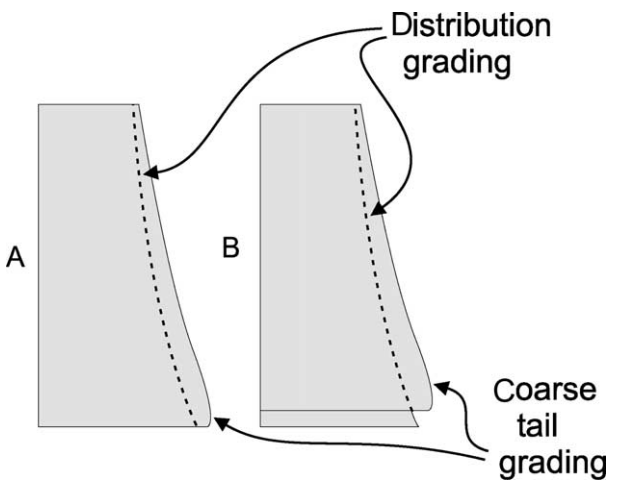


Fig. 9. Schematic graphic logs illustrating: (A) coarse tail grading developed in the case where coarser, head-derived and finer, body-derived material undergoes co-incident sedimentation; (B) a more complex vertical grading pattern produced due to earlier onset of sedimentation of finer, body-derived material.

possible that coarse tail grading might occur above a finer grained interval of approximately the same grain-size as the sandy matrix immediately above, which need not necessarily be inversely graded (Fig. 9B). It is worth noting that this pattern of grading differs from the inverse grading patterns predicted by Hand (1997) and those described by Mulder et al. (2003), which are interpreted to arise through coarse tail lag, and waxing flow, respectively. This is because the basal interval is characterised by a progressive inverse grading in these cases, rather than the abrupt coarsening shown in Fig. 9B.

## 7. Conclusions

Coherent spatial and temporal trends in velocity, grain-size and concentration are developed by flows, which originated from the quasi-steady input of uniform suspensions of sediment. The flow structures defined by these trends are, therefore, developed by the internal action of the flows themselves, and do not relate to the input condition. The occurrence of this progressive spatial evolution in flow structure implies that time series measured within such gravity currents may not be straightforwardly interpretable in terms of the instantaneous longitudinal current structure.

The quasi-steady input (limited duration) experimental currents produced flows which developed surge-type structures. Thus the history of flow steadiness as evidenced, for example, in the vertical grading structure of natural deposits, may not necessarily be indicative of the mechanism that generated the flow. Both current length and duration increase systematically along the length of the flume, indicating that a more rapid decline in velocity may occur proximally than distally. In natural flows, the duration of sedimentation may thus progressively increase along the flow distribution pathway, which may result in capacity-driven sedimentation (and hence massive sand deposition) being relatively more prevalent proximally and competence-driven sedimentation (and hence traction-dominated deposition) relatively more prevalent distally. In the experimental currents, an upward flux of coarse particles from the head can be inferred; these particles subsequently settle downwards into body. At the natural scale such a phenomenon may be responsible for the development of coarse tail grading.

## Acknowledgements

This work was carried out under the auspices of the Phase 3 Turbidites Project at Leeds University, supported by Amerada Hess, Anadarko, BG, BHP, BP, Chevron, Conoco, Elf, and Shell. We acknowledge the contribution of Jeff Peakall, whose overhead reservoir flow generation mechanism and 'sliding trolley' siphon sample collection equipment were adapted for use in these experiments.

## References

Allen, J. R. L. (1985). *Principles of physical sedimentology*. London: George Allen and Unwin.

Best, J. L., Kirkbride, A. D., & Peakall, J. (2001). Mean flow and turbulence structure of sediment-laden gravity currents: new insights using ultrasonic Doppler velocity profiling. In W. D. McCaffrey, B. C. Kneller, & J. Peakall (Eds.), *Particulate Gravity Currents Special Publication of the International Association of Sedimentologists* (pp. 159–172). Oxford: Blackwell Science Ltd.

Bonnecaze, R. T., Huppert, H. E., & Lister, J. R. (1993). Particle-driven gravity currents. *Journal of Fluid Mechanics*, *250*, 339–369.

Dade, W. B., & Huppert, H. E. (1995). A box model for non-entraining, suspension-driven gravity surges on horizontal surfaces. *Sedimentology*, *42*(3), 453–471.

Edwards, D. A. (1993). Turbidity currents: Dynamics, deposits and reversals. *Lecture Notes in Earth Sciences*, *44*, 173.

Felix, M. (2001). A two-dimensional numerical model for a turbidity current. In W. D. McCaffrey, B. C. Kneller, & J. Peakall (Eds.), *Particulate Gravity Currents Special Publication of the International Association of Sedimentologists* (pp. 71–81). Oxford: Blackwell Science Ltd.

Garcia, M. H. (1994). Depositional turbidity currents laden with poorly sorted sediment. *Journal of Hydraulic Engineering*, *120*(11), 1240–1263.

Gladstone, C., Phillips, J. C., & Sparks, R. S. J. (1998). Experiments on bidisperse, constant-volume gravity currents: Propagation and sediment deposition. *Sedimentology*, *45*(5), 833–843.

Hand, B. M. (1997). Inverse grading resulting from coarse-sediment transport lag. *Journal of Sedimentary Research*, *67*(1), 124–129.

Hiscott, R. N. (1994). Loss of capacity, not competence, as the fundamental process governing deposition from turbidity currents. *Journal of Sedimentary Research*, *64*, 209–214.

Imran, J., & Parker, G. (1999). On the role of mud in keeping sand in suspension in a turbidity current. *American Association of Petroleum Geologists 1999 Annual Meeting. American Association of Petroleum Geologists and Society of Economic Paleontologists and Mineralogists, Tulsa*, A66.

Kneller, B. C., Bennett, S. J., & McCaffrey, W. D. (1997). Velocity and turbulence structure of density currents and internal solitary waves: Potential sediment transport and the formation of wave ripples in deep water. *Sedimentary Geology*, *112*(3–4), 235–250.

Kneller, B. C., Bennett, S. J., & McCaffrey, W. D. (1999). Velocity structure, turbulence and fluid stresses in experimental gravity currents. *Journal of Geophysical Research*, *104*(C3), 5381–5391.

Kneller, B. C., & Branney, M. J. (1995). Sustained high-density turbidity currents and the deposition of thick massive sands. *Sedimentology*, *42*(4), 607–616.

Kneller, B., & McCaffrey, W. (1999). Depositional effects of flow nonuniformity and stratification within turbidity currents approaching a bounding slope: Deflection, reflection, and facies variation. *Journal of Sedimentary Research*, *69*(5), 980–991.

Kneller, B. C., & McCaffrey, W. D. (2003). The interpretation of vertical sequences in turbidite beds: the influence of longitudinal flow structure. *Journal of Sedimentary Research*, *73*, 706–713.

Lowe, D. R. (1982). Sediment gravity flows. II. Depositional models with special reference to the deposits of high-density turbidity currents. *Journal of Sedimentary Petrology*, *52*, 279–297.

Massey, B. S. (1989). *Mechanics of fluids*. London: Chapman&Hall, p. 599.

Middleton, G. V., & Southard, J. B. (1984). Mechanics of sediment movement. *SEPM*, Short Course 3, 401 pp.

Mulder, T., & Syvitski, J. P. M. (1995). Turbidity currents generated at river mouths during exceptional discharges to the world oceans. *Journal of Geology*, *103*, 285–299.

Mulder, T., Syvitski, J. P. M., Migeon, S., Faugeres, J. C., & Savoye, B. (2003). Marine hypopycnal flows, initiation, behaviour and related deposits: A review. *Marine and Petroleum Geology*, this issue (doi: 10.1016/SO264-8172(03)00127-2).

Pantin, H. M., & Leeder, M. R. (1987). Reverse flow in turbidity currents: The role of internal solitons. *Sedimentology*, *34*(6), 1143–1155.

Parker, G., Garcia, M., Fukushima, Y., & Yu, W. (1987). Experiments on turbidity currents over an erodible bed. *Journal of Hydraulic Research*, *25*(1), 123–147.

Parsons, J. D., & Garcia, M. H. (1998). Similarity of gravity current fronts. *Physics of Fluids*, *10*, 3209–3213.

Peakall, J., Ashworth, P., & Best, J. (1996). Physical modelling in fluvial geomorphology: Principles, applications and unresolved issues. *In: The Scientific Nature of Geomorphology: Proceedings of the 27th Binghamton Symposium in Geomorphology*, pp. 221–253.

Peakall, J., Felix, M., McCaffrey, B., & Kneller, B. (2001). Particulate gravity currents: Perspectives. In W. D. McCaffrey, B. C. Kneller, & J. Peakall (Eds.), *Particulate Gravity Currents, Special Publication of the International Association of Sedimentologists* (pp. 1–8). Oxford: Blackwell Science Ltd.

Simpson, J. E. (1997). *Gravity currents in the environment and the laboratory*. Cambridge: Cambridge University Press, 244 pp.

Stix, J. (2001). Flow evolution of experimental gravity currents: Implications for pyroclastic flows at volcanoes. *Journal of Geology*, *109*(3), 381–398.